CT-based tissue segmentation to assess knee joint inflammation and reactive bone formation assessed by ^{18}F-FDG and ^{18}F-NaF PET/CT: Effects of age and BMI

Abdullah Al-Zaghal[1] MD, Dani P. Yellanki[1], Cyrus Ayubcha[1], Thomas J. Werner[1] MSc, Poul F. Høilund-Carlsen[2,3] MD, DMSc, Abass Alavi[1] MD (Hon), PhD (Hon), DSc (Hon),

1. Department of Radiology, Hospital of University of Pennsylvania, PA, USA
2. Department of Nuclear Medicine, Odense University Hospital, Odense, Denmark
3. Institute of Clinical Research, University of Southern Denmark, Odense, Denmark

Keywords: ^{18}F-FDG - ^{18}F-NaF - Knee - Age - Obesity

Corresponding author:
Abass Alavi MD (Hon), PhD (Hon), DSc (Hon)
3400 Spruce St, Philadelphia, PA 19104
Office number: 215-662-3069
Fax number: 215-573-4107
abass.alavi@uphs.upenn.edu

Received:
21 June 2018
Accepted:
29 June 2018

Abstract

Objectives: This study was conducted to determine the role of computed tomography (CT)-based segmentation methodology to semi-quantify the degree of inflammation and reactive bone formation in the knee joints by fluorine-18-fluorodeoxyglucose (^{18}F-FDG) and ^{18}F-sodium fluoride positron emission tomography/CT (^{18}F-NaF PET/CT) imaging, respectively. Furthermore, we assessed the impact of aging and body mass index (BMI) on these biological responses. **Subjects and Methods:** In this retrospective study, we examined a total of 97 subjects who had undergone both ^{18}F-FDG and ^{18}F-NaF PET/CT scanning. The mean age was 49.3±14.9 (21-75) and the mean BMI was 26.7±4.3 (17.7-42.0). Whole joint compartments and osseous compartments were segmented on fused PET/CT images using a 3D-growing algorithm with an adjustable upper/lower Hounsfield Units (HU) thresholds and manual tools. The metabolic activity and volume of each compartment was measured, values from the osseous compartment were subtracted from the whole joint to get the volume and metabolic activity of the soft tissue. The metabolic activity was correlated with age and BMI. **Results:** Fluorine-18-FDG uptake in the soft tissues surrounding the joint was 0.35±0.07 while 0.19±0.04 in the osseous structures (P<0.0001). Aging positively correlated with ^{18}F-FDG uptake in the soft tissue (r=0.37, P=0.0001). Body mass index positively correlated with ^{18}F-FDG uptake in the soft tissue (r=0.53, P<0.0001), osseous compartment (r=0.58, P<0.0001) and ^{18}F-NaF uptake in the joint (r= 0.37, P=0.0001). A positive association was noted between the degree of new bone formation and the inflammatory reaction (P<0.01). **Conclusion:** The PET-based molecular imaging probes along with the CT-based segmentation techniques revealed an association between aging and the inflammatory activity of the soft tissue compartment. Similarly, a positive correlation was noted between BMI and inflammation and reactive bone formation of the knee joint compartments.

Hell J Nucl Med 2018; 21(2): 102-107 *Epub ahead of print: 12 July 2018* *Published online: 10 August 2018*

Introduction

The knee is the largest joint in the body and is comprised of two articulations: the tibiofemoral and the patellofemoral joints. Stability of the knee joint is governed by static and dynamic elements. Muscles acting on or across the knee provide the needed dynamic stability. Static stability is maintained by a combination of the ligaments, the menisci, the topography of the articular surface and the mechanical loads placed on the joint [1].

The average life expectancy is increasing worldwide [2], and knee disorders are a major cause of morbidity in the elderly population [3]. Chronic knee pain affects around 25% of adults and symptomatic osteoarthritis affects 12.1% of the US population [4, 5]. The prevalence of individuals undergoing total knee replacement reached up to 1.52% of the population in 2010 compared to 0.13% in 1980 [6].

Magnetic resonance imaging (MRI), ultrasonography, computerized tomography (CT), and plain radiographs are usually performed for the evaluation of symptomatic joints [7]. Positron emission tomography (PET) using fluorine-18-fludeoxyglucose (^{18}F-FDG) is a highly sensitive methodology for the early detection of inflammatory processes. Multiple studies using ^{18}F-sodium fluoride (NaF) PET imaging have been carried out for evaluating rheumatic diseases such as osteoarthritis and rheumatoid arthritis [8]. Based on these reports, it has been suggested that ^{18}F-NaF PET might provide the earliest evidence for metabolic changes and before structural changes become evident on MRI or other structural imaging modalities [9, 10].

This study was undertaken to determine the role of a CT-based methodology to segment the knee joint compartments and quantify its metabolic activity by PET techniques. We measured ^{18}F-FDG and ^{18}F-NaF uptake and compared the quantitative data with

two of the most important clinical risk factors for knee arthropathies: age and body mass index (BMI).

Patients and Methods

Fluorine-18-FDG and ^{18}F-NaF PET/CT scans utilized in this retrospective study are part of the "Cardiovascular Molecular Calcification Assessed by ^{18}F-NaF PET/CT" (CAMONA) protocol. CAMONA was a prospective study approved by the Danish National Committee on Biomedical Research Ethics, registered at ClinicalTrials.gov (NCT01724749), and conducted from 2012 to 2016 in accordance with the Declaration of Helsinki. Written informed consent was obtained from all study subjects. Detailed description of the CAMONA study was previously published by Blomberg BA et al. (2017) [11]

Subjects selection

The CAMONA study consists of 139 volunteers; 89 healthy subjects 50 subjects with history of chest pain. Healthy volunteers were recruited from the general population or from the blood bank of Odense University Hospital, Denmark. Subjects with a negative history of cardiovascular disease, oncologic disease, autoimmune disease, immunodeficiency syndromes, alcohol abuse, illicit drug use, or any prescription medication were considered as healthy volunteers. Framingham Risk Score was used to evaluate the modifiable cardiovascular risk factors and only subjects with score below the upper limits of the recommended levels were included [12]. Pregnant women were not included within the study population.

Subjects with history of chest pain were recruited from those whom were referred to the radiology department for a coronary CT-angiography. Only patients with a 10 years risk for fatal cardiovascular disease equal to or above 1%, as calculated by the BMI (kg/m^2) based Systematic Coronary Risk Evaluation (SCORE) tool, were eligible for inclusion. Subjects with a history of major cardiovascular events, malignancy, chronic inflammatory disease, illicit drug use, renal insufficiency were not included.

In the current study, 17 subjects that were excluded as the knee joints were not included within the field of imaging. Another 15 subjects that were excluded as either their ^{18}F-NaF or ^{18}F-FDG scan were not available within our lab database. Nine subjects were excluded due to technical issues that limited their scan analysis. One subject was excluded as due to prosthetic knee joint. A total of 97 subjects (69 normal subjects and 28 subjects with history of chest pain), 48 females and 49 males, were included (Table 1). Mean age was 49.36±14.95 years, range 21-75. Mean BMI was 26.73± 4.38kg/m^2, range 17.75-42.06. A linear correlation showed no significant relationship between subjects' age and their BMI; which allowed each variable to be independently assessed.

Study design

Information regarding subjects with smoking habits, family history of CVD, and prescription medication were acquired through questionnaires. Fasting serum total cholesterol, serum low-density lipoprotein (LDL) cholesterol, serum high-density lipoprotein (HDL) cholesterol, fasting plasma glucose and glycated hemoglobin (HbA1c) were measured. The estimated glomerular filtration rate (eGFR) was calculated using the Modification of Diet and Renal Disease (MDRD) equation. In each subject, the 10-year risk of developing CVD was approximated using the FRS based on age, gender, systolic blood pressure, total serum cholesterol, serum HDL cholesterol, smoking habit, and management for hypertension.

Table 1. *Subjects' demographics*

	Female	Male	P-value	Total (N=97)
	Total (n=48)	Total (n=49)		
Age (Years)	51.01± 15.10	47.6± 14.7	0.25	49.3± 14.9
Active smoking	2	6		8
BP (mmHg)				
Systolic	126.0± 17.8	132.1± 16.0	0.07	129.1± 17.1
Diastolic	75.5± 9.9	79.1± 8.3	0.05	77.4± 9.2
WBC (10^9/L)	5.8±1.7	6.3±1.6	0.16	6.1±1.7
BMI (Kg/m^2)	25.4± 3.5	27.9± 4.7	<0.01	26.9± 4.3
Creatinine (mmol/L)	72.8± 10.4	91.2± 17.6	<0.01	82.2± 17.1
MDRD-eGFR (mL/min/1.73m^2)	76± 13.3	80.2± 14.4	0.14	78.1± 14.0
Medication				
Lipid Lowering drugs	7	4		11
Antihypertensive drugs	7	9		16
Aspirin	2	5		7

BMI: Body Mass Index, BP: Blood Pressure, MDRD-eGFR: Glomerular Filtration Rate Estimated by the Modification of Diet and Renal Disease Formula, N: Sample size

The imaging protocol of the CAMONA study was previously published by Blomberg BA et al. (2014) [13, 14]. In summary, ^{18}F-FDG and ^{18}F-NaF PET/CT imaging were performed on hybrid PET/CT systems (GE Discovery STE, VCT, RX, and 690/710 systems (General Electric, Chicago, Illinois, USA)). Fluorine-18-FDG PET/CT imaging was performed 180 minutes after intravenous administration of 4.0MBq/kg, after an overnight fast of at least 8 hours and a confirmed blood glucose concentration of below 8mmol/L. On average, ^{18}F-NaF PET/CT imaging was performed within 14 days of ^{18}F-FDG PET/CT imaging. Fluorine-18-sodium fluoride PET/CT imaging was performed 90min after intravenous administration of 2.2MBq/Kg of ^{18}F-NaF. Positron emission tomography images were corrected for scatter, attenuation, random coincidences, and scanner dead time. Low-dose CT imaging (140 kV, 30-110mA, noise index 25, 0.8 second/rotation, slice thickness 3.75mm) was performed for attenuation correction and anatomical orientation. The effective radiation dose received from the entire imaging protocol was approximately 14mSv.

Image analysis

OsirX MD v.9.0 (DICOM viewer and image-analysis program, Pixmeo SARL; Bernex, Switzerland) was used for image analysis. Regions of interest (ROI) were manually assigned according to predetermined anatomical criteria. On a 3D maximum intensity projection (MIP) coronal view, midpoint between the lateral and the medial intercondylar tubercles was used as a landmark, then 2 lines parallel to the axial plane were drawn 4cm above and below to define the upper and lower borders of the knee joint, respectively.

Fluorine-18-FDG PET/CT images were segmented to measure the metabolic activity of the boney and surrounding soft tissue structures. For the whole joint segmentation, a 3D growing region algorithm with a lower Hounsfield Unit (HU) threshold of 90 was assigned on fused PET/CT images, followed by a morphological closing and dilatation algorithms with a structuring element radius of 20 and 5 units, respectively. The ROI included the femur, patella, and tibia along with the joint space, synovium and surrounding soft tissue (Figure 1). For the segmentation of the osseous part, ROI were manually assigned using a closed polygon tool and included the femur, patella, and tibia. The metabolic activity of the soft tissue was measured by subtracting the metabolic activity of the osseous part from the whole joint activity.

Only the osseous compartment was segmented on ^{18}F-NaF PET/CT images. A 3D growing region algorithm with a lower threshold of 150HU was applied, followed by a morphological closing algorithm with a structuring element radius of 15 units (Figure 2).

Mean standardized uptake value (SUVmean) and ROI_{volume} of both knees were measured for each trans-axial slice and exported to a CSV file by Osirix. Total metabolic activity of each slice was calculated by multiplying the slice SUVmean by the slice ROIvolume. The total metabolism of all slices was summed up to measure the total metabolic activity of the investigated tissue compartment, as in the following equation:

$$\text{Total Tissue Metabolism} = \sum (\text{Slice SUV}_{mean} * \text{Slice ROI}_{volume})$$

Total ^{18}F-FDG metabolism in the bone compartment was subtracted from the total ^{18}F-FDG metabolism in the whole joint to get the uptake in the soft tissue. Volume of the bone ROI was subtracted from the volume of the whole joint ROI to get the volume of the soft tissue.

Averaged SUVmean was used for the semi-quantification of ^{18}F-FDG and ^{18}F-NaF according to the following equation:

$$\text{Averaged SUV}_{mean} = \frac{\text{Total Tissue Metabolism}}{\text{ROI}_{total\_volume}}$$

To decrease the impact of adipose tissue on ^{18}F-FDG biodistribution during fasting state, SUVmean was corrected for lean body mass (SULmean). Tahari et al. (2014) reported that using Janmahasatian formulation annuls the bias caused by body weight on ^{18}F-FDG uptake by non-adipose tissue in females and decreases it in males [15]. Lean body mass (LBM) was calculated using Janmahasatian formulation [16]:

$$\text{LBM}_{janma} = \begin{cases} \dfrac{9.27 \times 10^3 \times \text{BW}}{6.68 \times 10^3 + 216 \times \text{BMI}} & \text{Men} \\ \dfrac{9.27 \times 10\text{^}3 \times \text{BW}}{8.78 \times 10\text{^}3 + 244 \times \text{BMI}} & \text{Women} \end{cases}$$

Averaged SULmean was calculated according to the following equation:

$$\text{Averaged SUL}_{mean} = \text{Averaged SUV}_{mean} \times \left(\frac{\text{LBM}_{janma}}{\text{Body Weight}}\right)$$

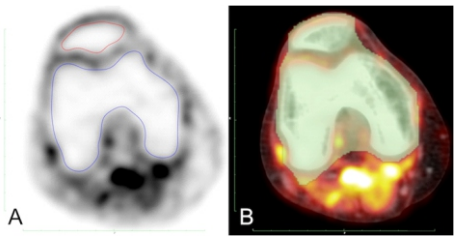

Figure 1. A) ROI manually assigned to include the femur and patella on an axial ^{18}F-FDG PET image using closed polygon tool. B) ROI of the whole joint on an axial fused ^{18}F-FDG PET/CT after applying a 3D growing algorithm with a lower threshold of 90HU followed by a morphological closing and dilatation algorithms with a struturing element radius of 20 units and 5 units, respectively.

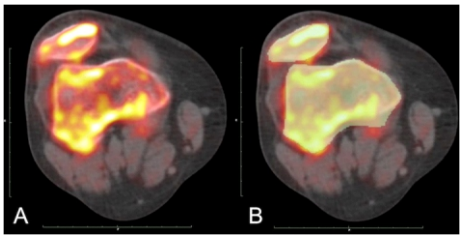

Figure 2. A) Trans-axial fused ^{18}F-NaF PET/CT images of the knee joint. B) Bone ROI highlighted after applying a 3D growing region algorithm with a lower threshold of 150HU and a morphological closing algorithm with a structuring element radius of 15.

Inter-operator agreement

Scans were independently analyzed by two investigators. Bland Altman plot was used to assess inter-operator agreement.

Statistical analysis

One-way ANOVA test, Pearson's correlation test, and linear regression analysis were used for parametric analysis. Statistical analysis was conducted using IBM SPSS Statistics version 25.0 (IBM Corp. Released 2017. IBM SPSS Statistics for Macintosh, Version 25.0. Armonk, NY: IBM Corp).

Results

For ^{18}F-FDG , mean of the averaged SUVmean was 0.35±0.07 in the whole joint, 0.19±0.04 in the osseous segment and 0.43±0.09 for in the soft tissues (P<0.0001), while mean of the averaged SULmean was 0.23±0.05 in the whole joint, 0.12±0.02 in the osseous segment and 0.29±0.06 in the soft tissue (P<0.0001). Mean ^{18}F-NaF uptake in the knee joint was 0.95±41.

A positive correlation was present between aging and the metabolic activity of ^{18}F-FDG in the soft tissue (SUV: r=0.37, P=0.0001. SUL: r=0.31, P=0.001), but no significant correlation was present with ^{18}F-FDG uptake in the osseous compartment (SUV: r=0.16, P=0.10. SUL: r=0.12, P=0.23). Significant associations were present between BMI and ^{18}F-FDG uptake in the soft tissue (SUV: r=0.53, P<0.0001. SUL: r=0.31, P= 0.001) as well as the osseous compartment (SUV: r=0.58, P< 0.0001. SUL: r=0.42, P<0.0001) (Figure 3). No correlation was noted between NaF uptake and aging (r=0.006, P=0.95), while a positive correlation was observed between ^{18}F-NaF uptake and BMI (r=0.37, P=0.0001) (Figure 4). Sodium fluoride uptake positively correlated with ^{18}F-FDG uptake in the bones (r=0.32, P=0.001) as well as the soft tissue (r=0.39, P< 0.0001) (Figure 5).

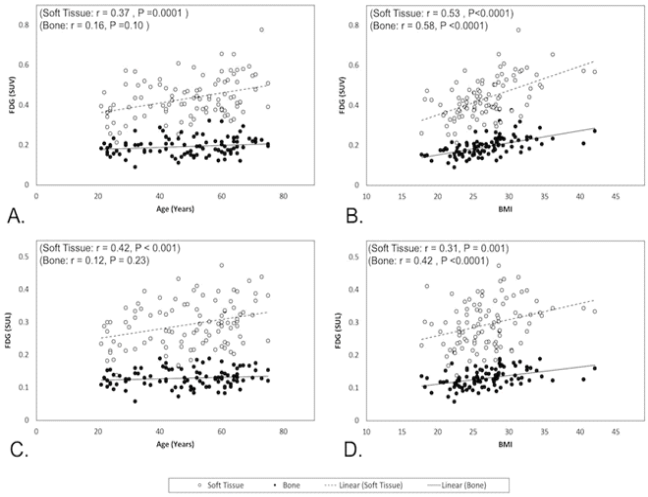

Figure 3. Aging positively correlating with ^{18}F-FDG uptake with in the soft tissue but not in the osseous compartment for both SUV (A) and SUL (C). Fluorine-18-FDG uptake positively correlated with BMI in the soft tissue and osseous compartments for both SUV (B) and SUL (D).

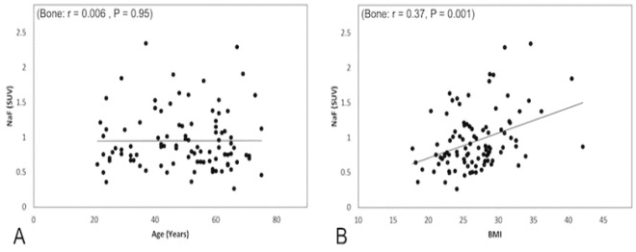

Figure 4. A) No association was found between the metabolic activity of ^{18}F-NaF in the knee joint and aging, B) Significant positive correlation was found between ^{18}F-NaF uptake in the knee joint with BMI.

The association between the differences of measurements conducted by both operators was not significant for ^{18}F-FDG activity in the soft tissue (r=0.14, P=0.15, range -0.04 to 0.05) and ^{18}F-NaF activity in the joint (r=0.11, P=0.28, range -0.18 to 0.12) (Figure 6). These findings indicate a strong inter-operator agreement.

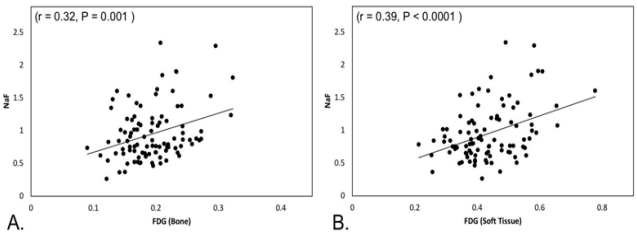

Figure 5. Significant trend of increasing NaF uptake with the inflammatory activity of the (A) osseous compartment and (B) the soft tissue compartment.

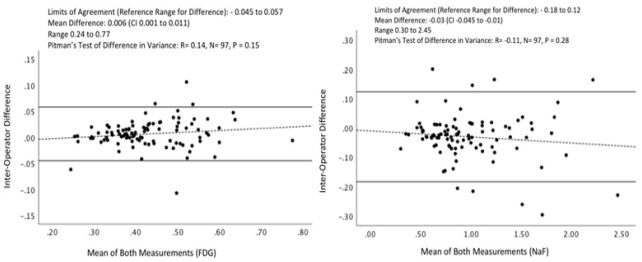

Figure 6. Measurements from both operators plotted on Bland-Altman charts. No significant proportional differences were observed for (A) ^{18}F-FDG uptake in soft tissue and (B) ^{18}F-NaF uptake in the joint.

Discussion

This scientific communication describes an approach to segment the joint compartments by using Hounsfield units on PET/CT, and such an approach leads to quantification of regional uptake of ^{18}F-FDG and ^{18}F-NaF in various structures.

The data generated from this study revealed a significant trend towards increasing degrees of ^{18}F-FDG uptake in the soft tissue compartment of the joint with both aging and high BMI. Interestingly, the results from the osseous structures showed a significant correlation between BMI and uptake of ^{18}F-FDG and ^{18}F-NaF, while no substantial changes were noted with aging. The degree of new bone formation was noted to have a significant positive association with the in-

flammatory activity (as noted by the degree of ^{18}F-FDG uptake) of both bone and soft tissue.

Musculoskeletal disorders pose a source of major health disabilities in the elderly. Osteoarthritis (OA) is a multi-factorial joint disorder that is related to both mechanical and inflammatory factors and is a major cause of morbidity in elderly subjects. Previously published studies have reported an association between knee joint inflammation and aging [17, 18].

Recent studies have described the influence of body weight in inducing and stimulating inflammatory reaction in the weight-bearing joints of obese subjects [19]. Chondrocytes have mechanoreceptors that sense changes in the exerted mechanical stress and translate it into biochemical signals, which consequently regulate the production of pro-inflammatory mediators [20, 21]. Mechanical strain and shear forces were also found to induce the production of COX-2, IL-2 and PGE2 in fibroblast-like synoviocytes [22]. Increasing compressive forces on subchondral bone was also associated with an increase in the expression of IL-6, COX-2 and IL-8 [23]. Infrapatellar fat pad also contributes to joint inflammation by the secretion of adipokines into the synovium [24]. The increase in the pro-inflammatory mediators keeps the joint in an active low-grade state of inflammation and continuous generation of reactive oxygen species (ROS) [25].

Adipose tissue secretes in obese subjects also secretes cytokines as TNF-a, leptin, IL-1, and IL-6 into systemic circulation [26]. Serum and synovial levels of leptin and IL-6 are associated with OA synovitis and positively correlated with the severity of degenerative changes on radiographs [27-29]. Osteophytes and chondrocytes were found to secrete leptin and IL-6 in advanced stages of OA [30].

Sodium fluoride uptake depends on the availability of hydroxyl ions (OH^-) on the surface of hydroxyl-apatite ($Ca_{10}[PO_4]_6[OH]_2$) in bone matrix and the suppling blood flow [31]. Conditions that alter bone metabolism whether by promoting bone formation or resorption lead to an increase in the surface area exposed to blood flow, thus, increasing ^{18}F-NaF uptake [32]. The increase in mechanical loading is associated with an increase in the proliferation and differentiation of osteoblasts and osteocytes, in turn increasing bone turnover [33-36].

Bone mass density declines with aging [37], and this affects the amount of hydroxyl-apatite in bone matrix, consequently decreasing the exposed surface area and binding sites available to react with ^{18}F-NaF. This might explain the absence of a correlation between aging and the activity of ^{18}F-NaF although it is common to find an increase in metabolic activity at site of new bone formation (osteophytes) in elderly.

The limitation of the study was due to a lack of relevant clinical information about subjects' history of knee pain or arthropathy. However, the main purpose of this research was to develop an analysis scheme for quantifying knee disorders with PET. As such, we are presenting a methodology to segment the knee joint compartments to assess various knee pathologies, aid in achieving an earlier disease diagnosis and provide an objective tool to follow disease activity as well as treatment response.

In conclusion, this scientific communication describes the role of PET-based molecular imaging and segmentation techniques in determining the metabolic activity of the knee joint compartments and the changes that occur due to aging and BMI. In particular, we are reporting an association between BMI and the inflammatory activity of the different knee joint compartments as well as bone turnover. Aging was also associated with an increase in the inflammatory of the knee soft tissue compartment. Our findings are consistent with the previously published studies regarding the impact of aging as well as BMI on the knee joint.

Financial disclosure

This study was funded by the Anna Marie and Christian Rasmussen's Memorial Foundation, University of Southern Denmark, Odense, Denmark, and the Jørgen and Gisela Thrane's Philanthropic Research Foundation, Broager, Denmark.

Acknowledgment

We thank the staff of the CAMONA study and the study participants for their valuable contributions

The authors declare that they have no conflicts of interest.

Bibliography

1. Flandry F, Hommel G. Normal anatomy and biomechanics of the knee. *Sports Med Arthrosc Rev* 2011; 19: 82-92.
2. Oeppen J, Vaupel JW. Broken limits to life expectancy. *Science* 2002; 296: 1029-31.
3. Fransen M, Simic M, Harmer AR. Determinants of MSK health and disability: lifestyle determinants of symptomatic osteoarthritis. *Best Pract Res Clin Rheumatol* 2014; 28: 435-60.
4. Nguyen U-SD, Zhang Y, Zhu Y et al. Increasing prevalence of knee pain and symptomatic knee osteoarthritis: survey and cohort data. *Ann Intern Med* 2011; 155: 725-32.
5. Luyten FP, Denti M, Filardo G et al. Definition and classification of early osteoarthritis of the knee. *Knee Surg Sports Traumatol Arthrosc* 2012; 20: 401-6.
6. Kremers HM, Larson DR, Crowson CS et al. Prevalence of total hip and knee replacement in the United States. *J Bone Joint Surg Am* 2015; 97: 1386-97.
7. Guermazi A, Alizai H, Crema M et al. Compositional MRI techniques for evaluation of cartilage degeneration in osteoarthritis. *Osteoarthritis Cartilage* 2015; 23: 1639-53.
8. Jadvar H, Desai B, Conti PS. Sodium ^{18}F-fluoride PET/CT of bone, joint, and other disorders. *Semin Nucl Med* 2015; 45: 58-65.
9. Raynor W, Houshmand S, Gholami S et al. Evolving role of molecular imaging with ^{18}F-sodium fluoride PET as a biomarker for calcium metabolism. *Curr Osteoporos Rep* 2016; 14: 115-25.
10. Kobayashi N, Inaba Y, Tateishi U et al. Comparison of ^{18}F-fluoride positron emission tomography and magnetic resonance imaging in evaluating early-stage osteoarthritis of the hip. *Nucl Med Commun* 2015; 36: 84-9.
11. Blomberg BA, De Jong PA, Thomassen A et al. Thoracic aorta calcification but not inflammation is associated with increased cardiovascular disease risk: results of the CAMONA study. *Eur J Nucl Med Mol Imag* 2017; 44: 249-58.
12. D'Agostino RB, Vasan RS, Pencina MJ et al. General cardiovascular risk profile for use in primary care: the Framingham Heart Study. *Circulation* 2008; 117: 743-53.
13. Blomberg BA, Thomassen A, Takx RA et al. Delayed ^{18}F-fluorodeoxyglucose PET/CT imaging improves quantitation of atherosclerotic plaque inflammation: results from the CAMONA study. *J Nucl Cardiol* 2014; 21: 588-97.
14. Blomberg BA, Thomassen A, Takx RA et al. Delayed sodium ^{18}F-fluoride PET/CT imaging does not improve quantification of vascular calcifica-

tion metabolism: Results from the CAMONA study. *J Nucl Cardiol* 2014; 21: 293-04.
15. Tahari AK, Chien D, Azadi JR, Wahl RL. Optimum lean body formulation for correction of standardized uptake value in PET imaging. *J Nucl Med* 2014; 55: 1481-4.
16. Janmahasatian S, Duffull SB, Ash S et al. Quantification of lean bodyweight. *Clin Pharmacokinet* 2005; 44: 1051-65.
17. Saboury B, Parsons MA, Moghbel M et al. Quantification of aging effects upon global knee inflammation by ^{18}F-FDG -PET. *Nucl Med Commun* 2016; 37: 254-8.
18. Hong YH, Kong EJ. (^{18}F) Fluoro-deoxy-D-glucose uptake of knee joints in the aspect of age-related osteoarthritis: a case-control study. *BMC Musculoskelet Disord* 2013; 14: 141.
19. Berenbaum F, Eymard F, Houard X. Osteoarthritis, inflammation and obesity. *Curr Opin Rheumatol* 2013; 25: 114-8.
20. Guilak F. Biomechanical factors in osteoarthritis. *Best Pract Res Clin Rheumatol* 2011; 25: 815-23.
21. Knapik DM, Perera P, Nam J et al. Mechanosignaling in bone health, trauma and inflammation. *Antioxid Redox Signal* 2014; 20: 970-85.
22. Takao M, Okinaga T, Ariyoshi W et al. Role of heme oxygenase-1 in inflammatory response induced by mechanical stretch in synovial cells. *Inflamm Res* 2011; 60: 861-7.
23. Sanchez C, Pesesse L, Gabay O et al. Regulation of subchondral bone ososteoblast metabolism by cyclic compression. *Arthritis Rheumatol* 2012; 64: 1193-203.
24. Ioan-Facsinay A, Kloppenburg M. An emerging player in knee osteoarthritis: the infrapatellar fat pad. *Arthritis Research & Therapy* 2013; 15: 225.
25. Sellam J, Berenbaum F. Is osteoarthritis a metabolic disease? *Joint Bone Spine* 2013; 80: 568-73.
26. Greene MA, Loeser RF. Aging-related inflammation in osteoarthritis. *Osteoarthritis Cartilage* 2015; 23: 1966-71.
27. Eaton CB. Obesity as a risk factor for osteoarthritis: mechanical versus metabolic. *Med Health R I* 2004; 87: 201-4.
28. Dumond H, Presle N, Terlain B et al. Evidence for a key role of leptin in osteoarthritis. *Arthritis Rheumatol* 2003; 48: 3118-29.
29. Ku JH, Lee CK, Joo BS et al. Correlation of synovial fluid leptin concentrations with the severity of osteoarthritis. *Clin Rheumatol* 2009; 28: 1431-5.
30. Stannus OP, Jones G, Quinn SJ et al. The association between leptin, interleukin-6, and hip radiographic osteoarthritis in older people: a cross-sectional study. *Arthritis Res Ther* 2010; 12: R95.
31. Costeas A, Woodard HQ, Laughlin JS. Depletion of ^{18}F from blood flowing through bone. *J Nucl Med* 1970; 11: 43-5.
32. Bastawrous S, Bhargava P, Behnia F et al. Newer PET application with an old tracer: role of ^{18}F-NaF skeletal PET/CT in oncologic practice. *Radiographics* 2014; 34: 1295-316.
33. Cao JJ. Effects of obesity on bone metabolism. *J Orthop Surg Res* 2011; 6: 30.
34. Markou P, Chatzopoulos D. Yttrium-90 silicate radiosynovectomy treatment of painful synovitis in knee osteoarthritis. Results after 6 months. *Hell J Nucl Med* 2009; 12: 33-6.
35. Chatzopoulos D, Markou P, Iakovou I. Scintigraphic imaging of knee synovitis in osteoarthritis after intra-articular injection of technetium-99m pertechnetate in the unilateral knee. *Hell J Nucl Med* 2006; 9: 69-71.
36. Sojan S, Bartholomeusz D. Cutaneous radiation necrosis as a complication of yttrium-90 synovectomy. *Hell J Nucl Med* 2005; 8: 58-9.
37. Black DM, Rosen CJ. Postmenopausal osteoporosis. *N Engl J Med* 2016; 374: 254-62.

Pablo Picasso. Child with a dove (1901). Oil in canvas. 73x54cm.